Orientation Behavior of the Three Principal Crystallographic Axes of Poly(butylene terephthalate) Estimated in Terms of Orientation Distribution Function of Crystallites

Masaru Matsuo,* Reiko Adachi, Xiaowen Jiang, and Yuezhen Bin

Textile and Apparel Science, Faculty of Human Life and Environment, Nara Women's University, Nara 630-8263, Japan

Received June 23, 2003; Revised Manuscript Received November 8, 2003

ABSTRACT: The orientation behavior of the three principal crystallographic axes, the *a*-, *b*-, and *c*-axes, was estimated in terms of the orientation distribution function for poly(butylene terephthalate) (PBT) crystallites with a triclinic unit cell. Despite a number of papers reported for the orientation of crytsallites, this paper is the first successful trial for a triclinic unit system. For crystalline polymers with a triclinic crystal unit, there are no crystal planes perpendicular to the *a*-, *b*-, and *c*-axes whose reflection cannot be detected by X-ray diffraction techniques. Accordingly, the functions of the *a*-, *b*-, and *c*-axes must be obtained from the method proposed by Roe and Krigbaum. In doing so, the orientation functions of the reciprocal lattice vectors must be measured by X-ray diffraction for a number of crystal planes. But the measurements are very difficult for crystalline polymers such as poly(ethylene terephthalate) (PET), nylon-66, and PBT with the triclinic crystal unit, since the orientation functions for a number of crystal planes are needed to calculate the orientation distribution function of *a*-, *b*-, and *c*-axes and the measurements are very difficult. Among the three polymers, PBT is the lowest crystallinity, and their diffraction intensities from most of crystal planes are very weak. Nevertheless, as the most difficult trial, the orientation of crystallites and the orientation of the *a*-, *b*-, and *c*-axes were carefully estimated for an uniaxially drawn PBT film in terms of orientation distribution function in order to check the limit of the estimations. As the successful result, it was found that the *c*-axes oriented affinely with respect to the stretching direction, and the *a*- and *b*-axes took a characteristic mode associated with the rotation of crystallites around their own *c*-axis.

Introduction

Polymer molecules are intrinsically anisotropic in physical properties such as mechanical and optical ones. The physical anisotropy in bulk in relation to the molecular orientation has been successfully used for manufacturing textile fibers and polymer films by means of mechanical drawing or rolling of the polymer aggregates uniaxially or biaxially. The evaluation for molecular orientation was proposed by Herman in terms of orientation factor.[1] This factor is a sort of the second moment of the orientation function. The estimation by orientation distribution function of crystallites was proposed by Roe and Krigbaum.[2−4] The mathematical representation was given by an expansion of the distribution function in a series of generalized spherical harmonics. This method has been very important to obtain the orientation of the three principal crystallographic axes, the *a*-, *b*-, and *c*-axes, of crystallites with a triclinic unit cell in terms of the orientation distribution function. Except a triclinic unit system, there are several papers for estimating orientation distribution functions of the three principal crystallographic axes, the *a*-, *b*-, and *c*-axes, of polyethylene,[3,5,6] poly(vinyl alcohol),[7,8] nylon-6,[9] and cellulose.[10]

For most of crystalline polymers with a triclinic unit cell, however, there are no crystal planes perpendicular to the *a*-, *b*-, and *c*-axes whose reflections can be detected directly by X-ray diffraction techniques. Accordingly, a number of the reciprocal lattice vectors of the crystal planes are needed to estimate the functions of the *a*-, *b*-, and *c*-axes by using the method proposed by Roe and Krigbaum.[2−4] The first trial was done for poly(ethylene terephthalate) films by Krigbaum and Balta.[11] However, the trial was perfectly unsuccessful since the accurate separation of an overlapped peak was impossible because of a weak X-ray source of their machine. Since then, there has been no paper for the orientation of crystallites with a triclinic unit cell.

Recently, Song[12] reported interesting phenomena that the orientations of their crystallites of PBT films prepared under different condition and stretched with different speeds were estimated in terms of the second-order orientation factors by using lattice parameters of the α and β forms proposed by Hall and Pass.[13] The characteristics were discussed in relation to the crystal size, lattice spacing, and mechanical properties. Another important papers for PBT have been published recently in manufacturing aspects for the processing[14−16] and the blends.[17]

Based on the current topics of PBT, this paper is concerned with the estimation of the three principal crystallographic axes, the *a*-, *b*-, and *c*-axes, of PBT film. Among crystalline polymers with a triclinic unit cell such as poly(ethylene terephthalate) (PET), nylon-66, and PBT, the evaluation for PBT is the most difficult because of the lowest crystallinity. But the recent development of a computer program for the separation of an overlapped peak and strong X-ray source provide a good evaluation of the orientation functions of the reciprocal lattice vectors of several crystal planes with high accuracy. Consequently, it becomes possible to calculate the orientation function of crystallites as well as the orientation functions of the *a*-, *b*-, and *c*-axes

* To whom all correspondence should be addressed: Fax 81-742-20-3462; e-mail m-matsuo@cc.nara-un.ac.jp.

10.1021/ma030347x CCC: $27.50
Published on Web 01/30/2004

Table 1. Crystallinity and Melting Points of PBT

draw ratio(λ)	crystallinity(%)	melting point(°C)
1.75	32	227
3.50	34	229

clearly on the basis of orientation functions of the reciprocal lattice vectors.

Experimental Section

PBT pellets were furnished from Mitsubishi Chemical Co. Ltd. The pellets of PBT were pressed at 250 °C under 0.5 MPa, and the molded specimen was immersed into ice water immediately. The thickness of all the specimens was about 600 μm. The film was cut into strips of length 50 mm and width 10 mm. The strips were placed in a hot oven at 200 °C for 5 min and then elongated to the desired draw ratios. After elongation, the specimens were maintained for 20 min to promote crystal transformation from the β form to the α form as much as possible and cooled to room temperature.

The weight crystallinity was calculated from the density measured by a pycnometer in chlorobenzene−carbon tetrachloride as a medium, by assuming the densities of crystalline and amorphous phases to be 1.396[18] and 1.282 g/cm^3,[19] respectively.

The melting point was estimated from the melting endotherms of the differential calorimerty (DSC) curves obtained at a constant heating rate of 10 °C/min. Table 1 shows the results. Very small increases in crystallinity and melting point were confirmed with increasing draw ratio.

The X-ray measurements were carried out using a 12 kW rotating anode X-ray generator (RDA-rA). By using the condition, the orientation distribution function of the reciprocal lattice vector of the jth crystal plane was estimated from the intensity distribution measured as a function of $2\theta_B$ (twice the Bragg angle) at a polar angle θ_j between the stretching direction and the reciprocal lattice vector of the jth crystal plane. The range of θ_j is from 0 to 90°. The intensity curve $I_{cry}(\theta_B,\theta_j)$ was decomposed into the contributions from the individual crystal planes, assuming that each peak is a symmetric Lorenzian function of $2\theta_B$ as shown in eq 1.

$$I_{cry}(\theta_B,\theta_j) = \sum_j \frac{I_j^\circ}{1 + (2\theta_0^j - 2\theta_B)^2/\beta_j^2} \quad (1)$$

where I_j^o is the maximum intensity of the jth peak, and $2\theta_B$ is the twice Bragg angle at which the maximum intensity of the jth peak appears.

By horizontal scanning of the diffraction counter as a function of $2\theta_B$ at a given polar angle θ_j, the intensity can be determined for the jth crystal plane (j = (110), (200), ...) may be given by[20]

$$2\pi q_j(\cos\theta_j) = \frac{\int_{2\theta_1}^{2\theta_2} I_{cry}(\theta_B,\theta_j)\, d\theta_B}{\int_0^\pi \int_{2\theta_1}^{2\theta_2} I_{cry}(\theta_B,\theta_j)\, d\theta_B \sin\theta_j\, d\theta_j} \quad (2)$$

where θ_1 and θ_2 are the Bragg angles at the two feet of an isolated diffraction peak after the peak separation. The orientation factor F_{l0}^j was expressed as

$$F_{l0}^j = \int_0^\pi 2\pi q_j(\cos\theta_j)\, P_l(\cos\theta_j)\, d\theta_j \quad (3)$$

Incidentally, the uniaxial orientation of crystallites with respect to the stretching direction was confirmed by X-ray diffraction pattern (end view) showing circular diffraction rings.

Theory

Following Roe and Krigbaum,[2−4] a complete mathematical description for the orientation of crystallites may be treated by using the orientation functions of the reciprocal lattice vectors of crystal planes. Figure 1 shows the geometrical interrelations of two Cartesian coordinates, $O-X_1X_2X_3$ and $O-U_1U_2U_3$ fixed within the bulk specimen and crystal structural unit, respectively. The orientation of the structural unit within the space of the film specimen may be specified by using three Euler angles, θ, ϕ, and η, as shown in diagram (a). The angles θ and ϕ, which define the orientation of U_3 axis of the unit within the space, are the polar and azimuthal angles, respectively, and η specifies the rotation of the unit around its own U_3 axis. The orientation of the jth axis with respect to the $O-X_1X_2X_3$ is given by the polar angle θ_j and the azimuthal angle ϕ_j as shown in column (b). Moreover, the jth axis within the structural unit is specified by the polar angle Θ_j and the azimuthal angle Φ_j shown in column (c).

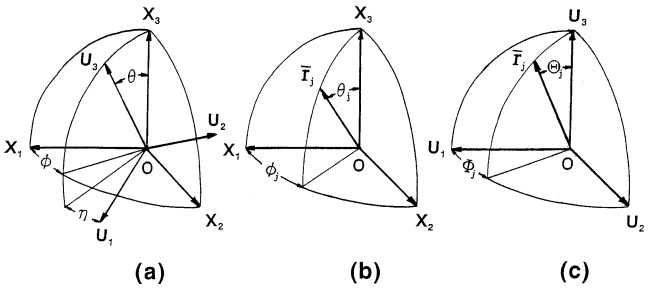

Figure 1. Cartesian coordinates illustrating the gometrical relation: (a) Euler angles θ and η which specify the orientation of coordinate $O-U_1U_2U_3$ of the structural unit with respect to coordinate $O-X_1X_2X_3$ of specimen. (b) Angles θ_j and φ_j which specify the orientation of the given jth axis of the structural unit with respect to the coordinate $O-X_1X_2X_3$. (c) Angles Θ_j and Φ_j which specify the orientation of jth axis of the structural unit with respect to the coordinate $O-U_1U_2U_3$.

In accordance with Roe's analysis,[4] the orientation distribution function $\omega(\theta,\phi,\eta)$ and $q_j(\cos\theta_j)$ may be expressed in a series of generalized spherical harmonics and spherical harmonics, respectively, as follows:

$$\omega(\theta,\phi,\eta) = \sum_{l=0}^{\infty}\sum_{m=-l}^{l}\sum_{n=-l}^{l} W^*_{lmn} Z_{lmn}(\xi) \exp\{-i(m\phi + n\eta)\} \quad (4)$$

and

$$q_j(\cos\theta_j) = \sum_{l=0}^{\infty}\sum_{m=-l}^{l} Q_{lm}^{j*} \prod_l^m (\xi_j) \exp\{-im\phi_j\} \quad (5)$$

where $\xi = \cos\theta$ and $\xi_j = \cos\theta_j$. W^*_{lmn} in eq 4 and Q_{lm}^{j*} in eq 5 are complex coefficients of the expanded series. They are given by

$$W^*_{lmn} = \frac{1}{4\pi^2}\int_{\eta=0}^{2\pi}\int_{\phi=0}^{2\pi}\int_{\theta=0}^{\pi} \omega(\theta,\phi,\eta)\, Z_{lmn}(\xi) \times \exp\{i(m\phi + n\eta)\} \sin\theta\, d\theta\, d\phi\, d\eta \quad (6)$$

and

$$Q_{lm}^{j*} = \frac{1}{2\pi}\int_{\phi_j=0}^{2\pi}\int_{\theta_j=0}^{\pi} q_j(\cos\theta_j,\phi_j) \prod_l^m (\xi_j) \times \exp(im\phi_j) \sin\theta_j\, d\theta_j\, d\phi_j \quad (7)$$

Here, $\omega(\theta,\phi,\eta)$ and $q_j(\cos\theta_j)$ are normalized orientation distribution functions of crystallites and the reciprocal

lattice vector $\mathbf{r}_j$ of the jth crystal plane, respectively. They are given by

$$\int_0^{2\pi}\int_0^{2\pi}\int_0^{\pi}\omega(\theta,\phi,\eta)\sin\theta\,\mathrm{d}\theta\,\mathrm{d}\phi\,\mathrm{d}\eta = 1 \tag{8}$$

and

$$\int_0^{2\pi}\int_0^{\pi} q_j(\cos\theta_j,\phi_j)\sin\theta_j\mathrm{d}\theta_j\,\mathrm{d}\phi_j = 1 \tag{9}$$

The function $Z_{lmn}(\xi)$ is given by[4,15]

$$Z_{lmn}(\xi) = \left\{\frac{2l+1}{2}\frac{(l-m)!}{(l-n)!}\frac{(l+m)!}{(l+n)!}\right\}^{1/2} \times \frac{1}{2^m}(1-\xi)^{2(m-n)}(1+\xi)^{(m+n)/2}P_{l-m}^{(m-n,m+n)}(\xi) \tag{10}$$

where $P_{l-m}^{(m-n,m+n)}(\xi)$ is a Jacobi polynomial.

The function $\Pi_l^m(\xi)$ is equivalent to $Z_{lm0}(\xi)$ at $n = 0$, which is the so-called normalized associated Legendre polynomial.

$$\prod_l^m(\zeta) = Z_{lm0}(\zeta) = \left\{\frac{2l+1}{2}\frac{(l-m)!}{(l+m)!}\right\}^{1/2} P_l^m(\zeta) \tag{11}$$

where $P_l^m(\zeta)$ is associated Legendre polynomials (not normalized).

Let us consider a given jth reciprocal vector $\mathbf{r}_j$ fixed within crystallite. The orientation of $\mathbf{r}_j$ may be specified by two sets of polar and azimuthal angles (θ_j, ϕ_j) and (Θ_j, Φ_j) with respect to the Coordinates, $O{-}X_1X_2X_3$ and $O{-}U_1U_2U_3$, respectively. The two sets of angles (θ_j, ϕ_j) and (Θ_j, Φ_j) referring to the vector $\mathbf{r}_j$ are related as

$$\begin{bmatrix}\sin\theta_j\cos\phi_j\\ \sin\theta_j\sin\phi_j\\ \cos\theta_j\end{bmatrix} = T(\theta,\phi,\eta)\begin{bmatrix}\sin\Theta_j\cos\Phi_j\\ \sin\Theta_j\sin\Phi_j\\ \cos\Theta_j\end{bmatrix} \tag{12}$$

where $T(\theta,\phi,\eta)$ is a linear transformation operator given by the following matrix:

$$T(\theta,\phi,\eta) = \begin{vmatrix}\cos\theta\cos\phi\cos\eta - \sin\phi\sin\eta & -\cos\theta\cos\phi\sin\eta - \sin\phi\cos\eta & \sin\theta\cos\phi\\ \cos\theta\sin\phi\cos\eta + \cos\phi\sin\eta & -\cos\theta\sin\phi\sin\eta + \cos\phi\cos\eta & \sin\theta\sin\phi\\ -\sin\theta\cos\eta & \sin\theta\sin\eta & \cos\theta\end{vmatrix} \tag{13}$$

With eq 13, a generalization of the Legendre addition theorem gives the following relations:

$$\prod_l^m(\zeta_i)\exp\{im\phi\} = \left(\frac{2}{2l+1}\right)^{1/2}\sum_{n=-l}^{l} Z_{lmn}(\xi) \times \exp\{i(m\phi+n\eta)\}\prod_l^n(\cos\Theta_j)\exp\{in\Phi_j\} \tag{14}$$

Multipying both sides of eq 12 by $\omega(\theta,\phi,\eta)$ and $q_j(\cos\theta_j)$ and integrating over all angles, θ, ϕ, η, θ_j, and ϕ_j, one can obtain the following relation:

$$Q_{lm}^{j*} = 2\pi\left\{\frac{2}{2l+1}\right\}^{1/2}\sum_{n=-l}^{l} W^*_{lmn}\prod_l^n(\cos\Theta_j)\exp\{in\Phi_j\} \tag{15}$$

The complex coefficients W^*_{lmn} in eq 4 and Q_{lm}^{j*} in eq 5 may be written as follows:

$$W^*_{lmn} = A_{lmn} + iB_{lmn} \tag{16-1}$$

$$Q_{lm}^{j*} = A_{lm}^j + iB_{lm}^j \tag{16-2}$$

For uniaxial stretching, unite vectors $\mathbf{U}_3$ and $\mathbf{r}_j$ take random orientation for ϕ and ϕ_j with respect to the X_3 and $m = 0$.

Considering the symmetric properties of $Z_{l0n}(\xi)$ with respect to the indice n, we have

$$Z_{l0n}(\xi) = Z_{l\bar{n}0}(\xi) = (-1)^n Z_{ln0}(\xi) = (-1)^n Z_{l0\bar{n}}(\xi) \tag{17}$$

and

$$\prod_l^n(\xi) = (-1)^n\prod_l^{\bar{n}}(\xi) \tag{18}$$

On the other hand, the Jacobi polynomials have the following symmetry with respect to the variable ξ

$$P_{l-n}^{(\alpha,\beta)}(\xi) = (-1)^{l-n}P_{l-n}^{(\beta,\alpha)}(-\xi) \tag{19}$$

so that

$$Z_{ln0}(\xi) = (-1)^{l-n}Z_{ln0}(\xi) \tag{20-1}$$

$$\prod_l^n(\xi) = (-1)^l\prod_l^{-n}(-\xi) = (-1)^{l+n}\prod_l^n(-\xi) \tag{20-2}$$

$$\Pi_l(\xi) = (-1)^l\Pi_l(-\xi) \tag{20-3}$$

We shall take the symmetries of the orientation distribution functions of $\boldsymbol{r}_j$ within the specimen as follows:

$$q_j(\cos\theta_j) = q_j(-\cos\theta_j) \tag{21}$$

In this case, l must be even. Hence B_{l0}^j must be zero.

Considering eqs 16−21, eq 15 reduces to

$$A_l^j = \{A_{l00}\Pi_l(\cos\Theta_j) + 2\sum_{n=1}^{l}(A_{l0n}\cos n\Phi_j - B_{l0n}\sin n\Phi_j)\prod_l^n(\cos\Theta_j)\} \tag{22}$$

Furthermore, eqs 4 and 5 reduce as follows:

$$\omega(\theta,\eta) = \sum_{l=0}^{\infty}A_{l00}\Pi_l(\xi) + \sum_{l=2}^{\infty}\sum_{n=1}^{l}(-1)^n(A_{l0n}\cos n\eta + B_{l0n}\sin n\eta)\prod_l^n(\xi) \tag{23}$$

and

$$q_j(\cos\theta_j) = \sum_{l=0}^{\infty}A_{l0}{}^j\Pi_l(\zeta_j) \tag{24}$$

The coefficients A_{l0n}, B_{l0n}, and A_{l0}^j may be considered as a sort of orientation factors, indicating an average degree of orientation distribution. To use the well-known description, one can define the generalized

orientation factors as follows:[21,22]

$$F_{l0n} = \left\{\frac{2l+1}{2}\frac{(l+n)!}{(l-n)!}\right\}^{1/2} 4\pi^2 A_{l0n} \qquad (25\text{-}1)$$

$$G_{l0n} = \left\{\frac{2l+1}{2}\frac{(l-n)!}{(l+n)!}\right\}^{1/2} 4\pi^2 B_{l0n} \qquad (25\text{-}2)$$

$$F^j_{l0} = \left\{\frac{2l+1}{2}\right\}^{1/2} 2\pi A^j_{l0} \qquad (25\text{-}3)$$

By using eq 25 and eq 11, eqs 22−24 may be rewritten as follows:

$$F^j_{l0} = F_{l00}P_l(\cos\Theta_j) + 2\sum_{n=1}^{l}\frac{(l-n)!}{(l+n)!}(F_{l0n}\cos n\Phi_j - G_{l0n}\sin n\Phi_j)P_l{}^n(\cos\Theta_j) \quad (26)$$

$$4\pi^2\omega(\theta,\eta) = \frac{1}{2} + 2\sum_{l=2}^{\infty}\left[\frac{2l+1}{2}\left\{F_{l00}P_l(\xi) + 2\sum_{n=1}^{l}\frac{(l-n)!}{(l+n)!}(F_{l0n}\cos n\eta + G_{l0n}\sin n\eta)P_l^n(\xi)\right\}\right] \quad (27)$$

and

$$2\pi q_j(\cos\theta_j) = \frac{1}{2} + 2\sum_{l=2}^{\infty}\frac{2l+1}{2}F^j_{l0}P_l(\xi_j) \qquad (28)$$

With F^j_{l0}, Θ_j, and Φ_j thus determined for the jth crystal plane, the coefficients F_{l0n} and G_{l0n} can be calculated by solving simultaneous equations of eq 26, changing j up to at least $2l+1$. In turn, the orientation distribution function of crystallites, $\omega(\theta,\eta)$ can be determined from eq 28 with the approximation of finite series of expansion up to $l = (j-1)/2$ (j: odd and l: even), instead of the infinite series of expansion. From experimental viewpoint, however, the measuring accuracy of $I_{cry}(2\theta_B,\theta_j)$ in eq 3 and, consequently, that of $q_j(\cos\theta_j)$ varies with j, so that the simultaneous equations must be solved by use of a weightened least-squared method, as proposed by Roe and Krigbaum.[2,3]

In the case of the orthorhombic unit like polyethylene, a given vector $\mathbf{r}_j$ at Θ_j and Φ_j is equivalent to following seven vectors: $\mathbf{r}_j$ (1) at Θ_j and $-\Phi_j$, (2) at Θ_j and $\pi-\Phi_j$, (3) at Θ_j and $\pi+\Phi_j$, (4) at $\pi-\Theta_j$ and Φ_j, (5) at $\pi-\Theta_j$ and $-\Phi_j$, (6) at $\pi-\Theta_j$ and $\pi+\Phi_j$, (7) at $\pi-\Theta_j$ and $\pi-\Phi_j$. Accordingly, n must be even, and consequently G_{l0n} becomes zero. Thus, eqs 26 and 27 reduce to[6]

$$F^j_{l0} = F_{l00}P_l(\cos\Theta_j) + 2\sum_{n=2}^{l}\frac{(l-n)!}{(l+n)!}F_{l0n}P_l^n(\cos\Theta_j)\cos n\Phi_j \quad (29)$$

and

$$4\pi^2\omega(\theta,\eta) = \frac{1}{2} + 2\sum_{l=2}^{\infty}\left[\frac{2l+1}{2}F_{l00}P_l(\xi) + 2\sum_{n=2}^{l}\frac{(l-n)!}{(l+n)!}F_{l0n}P_l^n(\xi)\cos n\eta\right] \quad (30)$$

For a monoclinic crystal unit like polypropylene ($\beta \neq 90°$), G_{l0n} becomes zero, and eqs 26 and 27 reduce to

$$F^j_{l0} = F_{l00}P_l(\cos\Theta_j) + 2\sum_{l=1}^{\infty}\frac{(l-n)!}{(l+n)!}F_{l0n}P_l^n(\cos\Theta_j)\cos n\Phi \quad (31)$$

and

$$4\pi^2\omega(\theta,\eta) = \frac{1}{2} + 2\sum_{l=2}^{\infty}\left[\frac{2l+1}{2}F_{l00}P_l(\xi) + 2\sum_{n=1}^{l}\frac{(l-n)!}{(l+n)!}F_{l0n}P_l^n(\xi)\cos n\eta\right] \quad (32)$$

On the other hand, for a monoclinic crystal unit ($\gamma \neq 90°$) like poly(vinyl alcohol),[7,8] cellulose,[10] and nylon-6,[9] n must be even, and eqs 26 and 27 reduce to

$$F^j_{l0} = F_{l00}P_l(\cos\Theta_j) + 2\sum_{l=2}^{\infty}\frac{(l-n)!}{(l+n)!}(F_{l0n}\cos n\Phi_j - G_{l0n}\sin n\Phi_j)P_l^n(\cos\Theta_j) \quad (33)$$

and

$$4\pi^2\omega(\theta,\eta) = \frac{1}{2} + 2\sum_{l=2}^{\infty}\left[\frac{2l+1}{2}\left\{F_{l00}P_l(\xi) + 2\sum_{n=2}^{l}\frac{(l-n)!}{(l+n)!}(F_{l0n}\cos n\eta + G_{l0n}\sin n\eta)P_l^n(\xi)\right\}\right] \quad (34)$$

The function $2\pi q_j(\cos\theta_j)$ is available directly using X-ray diffraction techniques as described in eq 2, and the orientation factor F^j_{l0} may be obtained from eq 3. Substituting experimental F^j_{l0} into eq 26, we can obtain the generalized orientation factors F_{l0n} and G_{l0n} by solving the linear system of eq 26. As discussed before, Θ_j and Φ_j in eq 26 are known parameters for every crystal plane and for the three principal crystallographic axes, the a- , b-, and c-axes, since they are polar and azimuthal angles specifying the orientation of the reciprocal lattice vector with respect to the Cartesian coordinate of a crystal unit. Namely, the lth-order orientation factors, F_{l0n} and G_{l0n}, for a triclinic crystal unit may be determined, when the orientation factors F^j_{l0} can be obtained for the crystal planes of the number of $(2l+1)$ (see eq 26).

For a monoclinic crystal unit like polypropylene, the lth-order orientation factors, F_{l0n} (l; even and odd), may be obtained by measuring the orientation factors F^j_{l0} concerning $(l+1)$ crystal planes (see eq 31). For poly(vinyl alcohol) and nylon-6, the lth-order orientation factors, F_{l0n} and G_{l0n} (l; even), may be determined by measuring the orientation factors F^j_{l0} concerning the crystal planes of the number of $(l+1)$ (see eq 33). As reported by a number of papers,[3,5,6] F_{l0n} (l; even) for an orthorhombic unit like polyethylene may be determined by measuring the orientation factors F^j_{l0} concerning $(l/2+1)$ crystal planes (see eq 29).

Here it should be noted that the series expansion becomes higher as the distribution of $2\pi q_j(\cos\theta_j)$ becomes sharper. Accordingly, the estimation of the orientation distribution functions of the a-, b-, and c-axes becomes most complicated for a triclinic crystal unit. This indicates that the estimation becomes impos-

sible for the highly oriented films. This shall be discussed later in detail.

Now, we shall discuss the popular treatment for a triclinic crystal unit. The second-order orientation factor, F_{20n} and G_{20n} (at $l = 2$ in eq 26), can be obtained by eq 35, when the factor F^j_{20} can be obtained for five crystal planes.[17]

$$F^j_{20} = F_{200}P_2(\cos\Theta_j) + 2\sum_{n=1}^{2}\frac{(2-n)!}{(2+n)!}(F_{20n}\cos n\Phi_j - G_{20n}\sin n\Phi_j)P^n_2(\cos\Theta_j) \quad (35)$$

This means that the second-order orientation factors of three principal crystallographic axes, the *a*- , *b*-, and *c*-axes, which cannot be measured by the X-ray diffraction technique, can be obtained from the second-order orientation factors of five crystal planes with high diffraction intensity. In other words, this estimation must be adopted for the evaluation of the second-order orientation factor of the *a*-, *b*-, and *c*-axes of a triclinic crystal unit such as PET, PBT, and nylon-66. Even so, most of the estimations[23] have been carried out by using a sort of convenient method that was proposed by Wilchinsky.[24] The estimation is essentially wrong. Incidentally, the orientation factors of the *a*-, *b*-, and *c*-axes for monoclinic and orthorhombic units can be estimated from F^j_{l0} measured for three and two crystal planes, respectively, in accordance with Wilchinsky's method.[24]

In accordance with the mathematical treatment described before, the orientation distribution function of large number of crystal planes must be measured by the X-ray diffraction technique to obtain the orientation distribution of the *a*-, *b*-, and *c*-axes of PET and PBT with a triclinic crystal unit from the orientation distribution function of crystallites. This paper, as the most difficult example, deals with the trial for evaluating the orientation functions of the *a*-, *b*-, and *c*-axes of a drawn PBT film.

Results and Discussion

In actual estimation of the orientation distribution function of crystallites, we must consider the difficulty in carrying out peak separation by eq 1. Namely, there are some crystal planes whose Bragg angle reflections are located very close to each other. If the *j*th overlapped peak contains crystal planes with the number of *i*, the composed function $q_j(\cos\theta_j)$ includes the contribution of several planes as follows:

$$2\pi q_j(\cos\theta_j) = 2\pi\sum_{i=1}^{N_i}C_{ji}q_{ji}(\cos\theta_j) \quad (36)$$

The concept underlying eq 36 was first presented by Roe and Krigbaum.[2,3] N_i is the number of the peak separated from *j*th superposed peak, and C_{ji} is the relative (normalized) weight for the vector $\mathbf{r}_{ji}$. Before the numerical calculation by computer, initial values of C_{ji} are given by

$$C_{ji} = \frac{F_{ji}}{\sum_{i=1}^{N_i}F_{ji}} \quad (37)$$

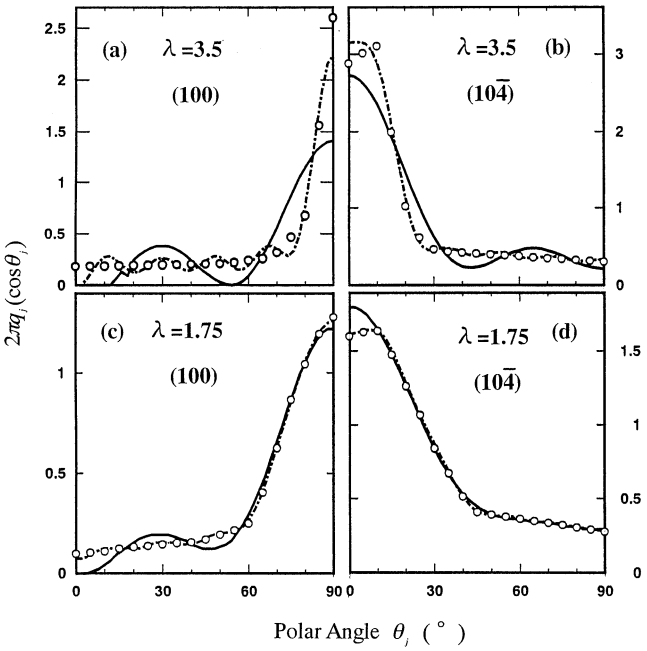

Figure 2. Orientation distribution function $2\pi q_j(\cos\theta_j)$ of the (100) and (10$\bar{4}$) planes of PBT films with $\lambda = 1.75$ and 3.5: (open circles) observed results; (solid curves) calculated by seires expansion up to $l = 6$, and (dotted curve) up to $l = 18$.

where F_{ji} is the structure factor of the *i*th crystal plane separated from the *j*th overlapped peak. In this case, eq 26 may be rewritten as follows:

$$F^j_{l0} = F_{l00}\sum_{i=1}^{N_i}C_{ji}P_l(\cos\Theta_j) + 2\sum_{n=1}^{l}\frac{(l-n)!}{(l+n)!}(F_{l0n}\sum_{i=1}^{N_i}C_{ji}P^n_l(\cos\Theta_{ji})\cos n\Phi_{ji} - G_{l0n}\sum_{i=1}^{N_i}C_{ji}P^n_l(\cos\Theta_{ji})\sin n\Phi_{ji}) \quad (38)$$

The individual functions $2\pi q_j(\cos\theta_j)$ can be obtained for 11 crystal planes, and the superposed function was obtained for a overlapped peak of the (101) and (012) planes. The estimation for the other crystal planes was impossible, and then the number of *j* (the number of crystal planes) becomes 13. In this case, series expansion in eq 26 cannot be beyond $l = 6$ to solve eq 38. Such few series expansion contains a big restriction for determining the curve profile of $2\pi q_j(\cos\theta_j)$. Namely, the experimental curves of $2\pi\, q_j(\cos\theta_j)$ must be smooth.

Figure 2 shows the observed and calculated $2\pi q_j(\cos\theta_j)$ of the (100) and (10$\bar{4}$) planes measured for the specimens with $\lambda = 1.75$ and 3.5. The observed curves represent as open circles. The solid and dotted curves are obtained by series expansion up to $l = 6$ and 18, respectively. The calculated curves can be obtained by using eqs 1−3 and eq 28. The good agreement between the experimental and calculated curves can be achieved by the expansion up to $l = 18$, when the experimental curves show sharp profile. However, the series expansion must be terminated up to $l = 6$, since PBT films with crystallinity less than 33%, cannot provide the distributions of $2\pi q_j(\cos\theta_j)$ for more than 13 crystal planes. This indicates that the orientation of crystallites for the specimen with $\lambda = 3.5$ cannot be evaluated since series expansion needs up to higher order to achieve

Table 2. Diffraction Angle $2\theta_B$, Polar Angle Θ_j, Azimuthal Angle Φ_j, the Weighting Factor ρ_j, and the Second-Order Orientation Factor

crystal plane	$2\theta_B$	Θ_j	Φ_j	F^j_{20}	ρ_j
(100)	23.38	90.00	0.00	−0.2980	1.0000
(1$\bar{1}$1)	25.35	68.35	324.87	−0.2860	1.0000
(010)	17.25	90.00	61.41	−0.3880	1.0000
(01$\bar{1}$)	16.17	61.78	103.97	−0.2410	0.2920
(110)	21.60	90.00	314.44	−0.3170	0.0661
(101)	19.90	67.36	4.09	−0.3120	0.0842
(012)	19.85	39.48	276.25	0.0180	0.0157
(112)	24.10	50.43	106.40	0.0968	0.1261
(111)	20.77	68.35	121.39	−0.0983	0.0788
(01$\bar{1}$)	22.42	69.99	51.54	−0.2800	0.0586
(104)	31.50	11.99	306.39	0.4100	0.2130
(001)	9.11	33.10	15.20	0.1470	0.6260
(01$\bar{3}$)	26.42	29.17	118.86	0.4790	0.1170
a-axis		60.48	335.92	−0.2350	
b-axis		90.00	90.00	−0.2750	
c-axis		9.70	270.00	0.4670	
c′-axis		0.00	0.00	0.5730	

good curve fitting for $2\pi q_j(\cos\theta_j)$ with a sharp profile. Accordingly, the following evaluation is done only for the specimen with $\lambda = 1.75$. This is the very serious problems for crystalline polymers with a triclinic crystal unit. As for polyethylene, 13 crystal planes allow the series expansion up to $l = 24$, which is enough to reappear $2\pi q_j(\cos\theta_j)$.

As a first step, the generalized orientation factors F_{l0n} and G_{l0n} must be determine by solving eq 38 based on a least-squares method. In doing so, the needed values of Θ_j and Φ_j can be obtained from a crystal unit of PBT as have been proposed by Yokouchi et al.,[25] Hall et al.,[13] and Desborough et al.[26] In this paper, the values are listed in Table 2, which were calculated by a crystal unit of α form proposed by Yokouchi et al.[25] Thus, F^j_{l0} calculated from F_{l0n} and G_{l0n} by eq 38 lead to $2\pi q_j(\cos\theta_j)$ by using eq 28. The resulting calculated curves must be in good agreement with the curves calculated from eq 2 obtained experimentally by X-ray diffraction measurements. Namely, one must confirm the accuracy of the experimental data. For this purpose, weighting factors ρ_j were assumed initially to be nearly proportional to square of the structure factor and were subsequently varied to obtain the best fit between experimental and calculated results by the simplex method.[27] In actual calculation by computer, ρ_j is fixed to be unity for the (110), (1$\bar{1}$1), and (010) planes with strong diffraction intensity. A mean-square error R between the calculated factor $(F^j_{l0})_{cal}$ and recalculated factor $(F^j_{l0})_{recal}$ was obtained using

$$R = \frac{\sum_j \sum_l \rho_j[(F^j_{l0})_{cal} - (F^j_{l0})_{recal}]}{\sum_j \sum_l \rho_j[(F^j_{l0})_{cal}]} \qquad (39)$$

As described above, we recalculated F^j_{l0}, in turn, from the values of F_{l0n} and G_{l0n}, assuring the minimized value of R in eq 39 by best fitting of ρ_j and further calculated $2\pi q_j(\cos\theta_j)$. The value of R in eq 39 was 11.5%. The values of ρ_j are listed in Table 2.

Figure 3 shows the observed orientation functions of $2\pi q_j(\cos\theta_j)$ (open circles) and the recalculated functions (solid curves). It is evident that fairly good agreement between observed and recalculated distribution functions was observed, even for the less accurately crystal planes with lower weighting factors. The slight disagreement is due to termination error of the spherical harmonics up to $l = 6$. To achieve better agreement between observed and recalculated curves, series expansion needed must be higher order than $l = 6$. As discussed before, it is impossible to obtain more than 17 curves of $2\pi q_j(\cos\theta_j)$ for the present PBT specimen with low crystallinity.

Figure 4a shows the orientation distribution function of crystallites $\omega(\theta,\eta)$ calculated from eq 27 by using the coefficients F_{l0n} and G_{l0n} which are determined from eq 38 with l limited to 6. As can be seen from this figure, several highly populated regions exist, which complicate the detailed analysis of the orientation mode of crystallites of PBT. Namely, in the range of η from 0 to 360°, $\omega(\theta,\eta)$ shows a considerable dependence of η, having abnormal populated regions around $\eta = 20$, 130, 200, and 280°. These regions must be artifacts of expansion of $2\pi q_j(\cos\theta_j)$ into infinite series of spherical harmonics. Hence, the real distribution is shown in Figure 4b after eliminating the artifacts. The maximum population of $\omega(\theta,\eta)$ appears at $\theta = 0°$. This is surely real population characterizing the orientation of PBT crystallites under uniaxially elongation. The profile indicates that the orientation of PBT crystallites is out of the framework of a floating model associated with affine mode. If orientation follows affine mode, the contour map with maximum population shows a circular profile independent of η. Namely, such considerable η dependence is due to the specific rotation of crystallites around the *c*-axis as has been observed for the orientation of crystallites of poly(vinyl alcohol)[7,8] and nylon-6[9] films. If $\omega(\theta,\eta)$ shows a circular contour map having a maximum peak at $\theta = 0°$ showing a random rotation of crystallites around their *c*-axis, all $2\pi q_j(\cos\theta_j)$ of the (hk0) plane showed the same curves.

The orientation distribution functions of the *a*-, *b*-, and *c*-axes in addition to the *c*′-axis perpendicular to the *a*−*b* plane can be determined by substituting the values of Θ_j and Φ_j for each axis (listed in Table 2) into eq 26 and by using eq 27. Figure 5 shows the results. The functions of the *c*- and *c*′-axes show a monotonous decreasing curve, indicating the simple preferential orientation with respect to the stretching direction. The functions of the *a*- and *b*-axes have two peaks at $\theta_j = 0$ and 90° and a valley around at $\theta_j = 35°$, which indicates two rotational modes of crystallites around their *c*-axis.

Finally, we shall check whether the orientation of the *c*-axes follows an affine fashion given by the following equation:[28]

$$\omega(\theta) = \frac{\lambda^3}{2\{\lambda^3 - (\lambda^3 - 1)\cos^2\theta\}^{3/2}} \qquad (40)$$

Figure 6 shows the results. The curves show a peak at $\theta_j = 0°$ and the peak becomes shaper with increasing draw ratio of λ. It is seen that the function at $\lambda = 1.75$ is in good agreement with that of the *c*-axis shown in Figure 5. This indicates that the orientation of the *c*-axes follows a floating model associated with an affine mode and the *a*- and *b*-axes take characteristic rotation around the *c*-axis. Such rotation is probably thought to be due to the deformation of superstructure like spherulites characterizing untwisting of crystal lamella and reorientation of crystallites within the lamella. The good agreement between observed and recalculated $2\pi q_j(\cos\theta_j)$ is very important to assure the accuracy of observed

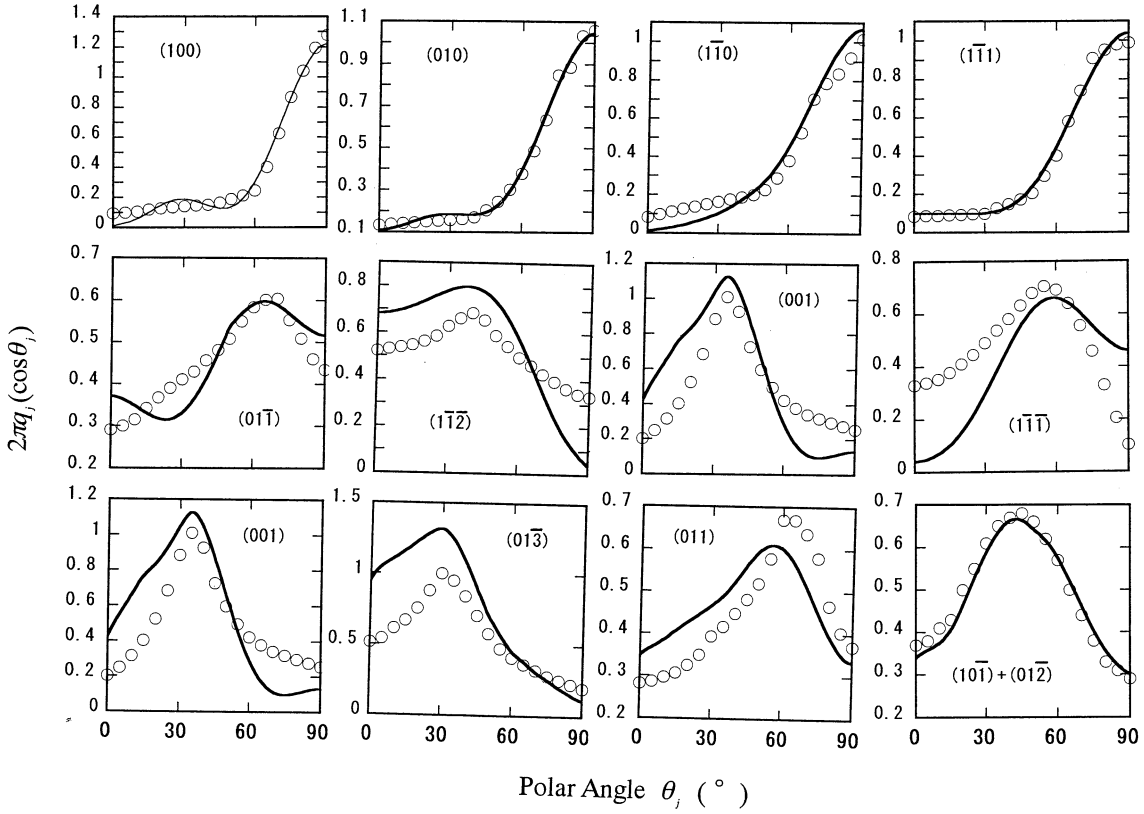

Figure 3. Observed orientation functions of $2\pi q_j(\cos\theta_j)$ (open circles) and the recalculated functions (solid curves) for the indicated crystal planes of a PBT film with $\lambda = 1.75$.

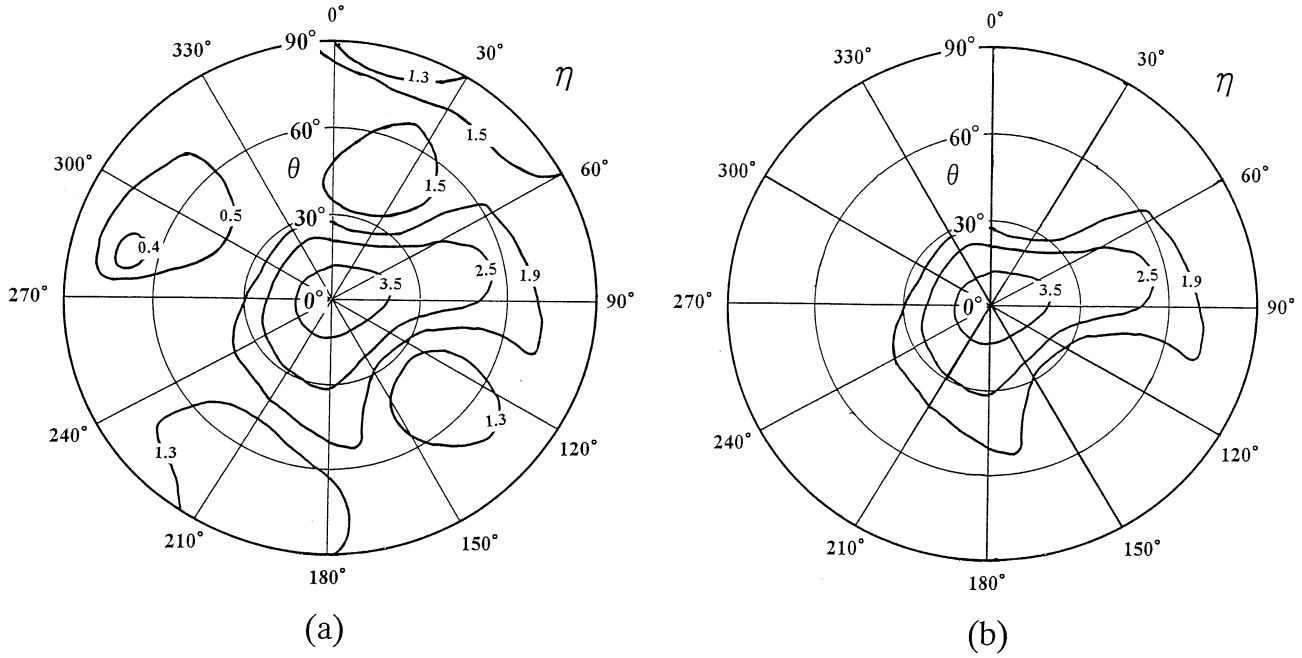

Figure 4. Orientation distribution function $\omega(\theta,\eta)$ of crystallites of a PBT film with $\lambda = 1.75$: (a) $\omega(\theta,\eta)$ calculated from eq 7 directly; (b) $\omega(\theta,\eta)$ eliminating artificial error.

results of $2\pi q_j(\cos\theta_j)$. Furthermore, the accuracy of the values of the second and fourth moments, F_{l0n} and G_{l0n}, provides the clear relationship between Young's modulus and orientation distribution of crystallites. Namely, the relationship between crystalline compliance (and/or stiffness) and molecular orientation can be formulated by using the fourth-order moments, F_{l0n} and G_{l0n}, if a polymeric system is perfectly crystalline. For actual polycrystalline systems, the fourth-order orientation factor F_{l0n} ($2 \le l \le 4$) for amorphous chain segments are needed in addition to F_{l0n} ($2 \le l \le 4$ and $0 \le n \le 4$) and G_{l0n} ($2 \le l \le 4$ and $0 \le n \le 4$) of crystallites to calculated Young's modulus in films and fibers as a function of crystallinity on the basis of the composite structural model.[29,30] However, birefringence and infrared and dye dichroisms provide only the second-order orientation factor.[31] On the other hand, polarized fluorescence provides the fourth-order orientation factor of

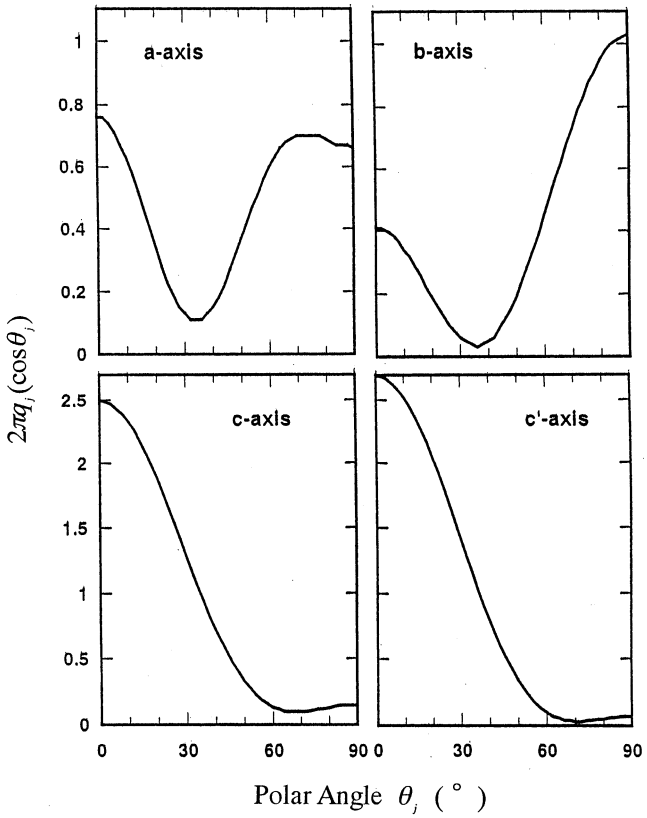

Figure 5. Orientation distribution functions of the *a*-, *b*-, and *c*-axes in addition to the axis perpendicular to the *a*−*b* plane of a PBT film with $\lambda = 1.75$.

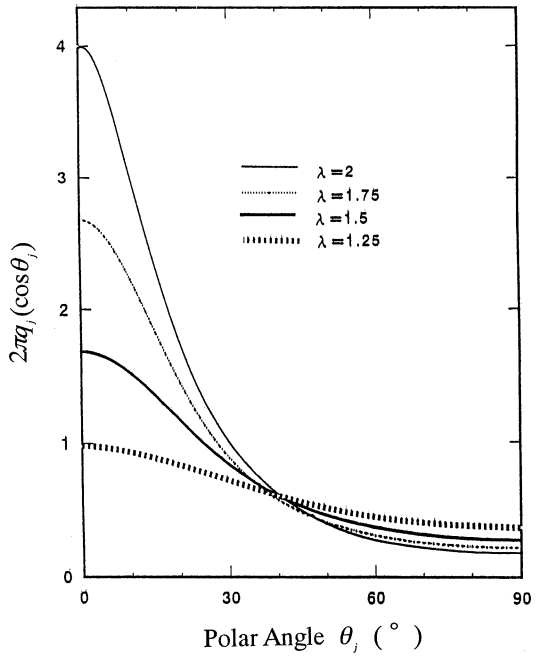

Figure 6. Orientation distribution function calculated by a floating model at the indicated λ.

amorphous chain segments. The polarized fluorescence was first applied to the estimation of molecular orientation by Nishijima et al.,[32] and the theoretical estimation was done by Kimura et al.[33] The further development was done by Monnerie and Jarry, and their method was applied to the detailed estimations of amorphous chain orientation of polypropylene[34] and PET.[35]

Finally, we must emphasize again that the estimation for the orientation distribution function of crystallites as well as the functions of the *a*-, *b*-, and *c*-axes for drawn PET and nylon-66 films is expected to be much easier than that for drawn PBT films because of their higher crystallinity.

Conclusion

The orientation of crystallites with a triclinic crystal unit was evaluated in terms of orientation distribution function, and the numerical calculation was carried out for a PBT film elongated uniaxially. The orientation distribution function $\omega(\theta,\eta)$ of crystallites was calculated by using the functions of the reciprocal lattice vectors of 13 crystal planes. The functions of the reciprocal lattice vectors were recalculated from $\omega(\theta,\eta)$. The recalculated functions were fairly in good agreement with the observed ones. The orientation of three principal crystallographic axes, *a*-, *b*-, and *c*-axes could be evaluated in terms of the orientation distribution function. As a result, the orientation of the *c*-axes oriented affinely with respect to the stretching direction and the *a*- and *b*-axes took a characteristic mode associated with the rotation of crystallites around their own *c*-axis. This is probably attributed to the characteristic deformation of superstructure like spherulites and/or rods associated with untwisting of crystal lamella and reorientation of crystallites within the lamella.

References and Notes

(1) Herman, P. H. *Physics and Chemistry of Cellulose Fibers*; Elsevier: New York, 1949; Vol. 255, p 393.
(2) Roe, R. J.; Krigbaum, W. R. *J. Chem. Phys.* **1964**, *40*, 2608.
(3) Krigbaum, W. R.; Roe, R. J. *J. Chem. Phys.* **1964**, *41*, 737.
(4) Roe, R. J. *J. Appl. Phys.* **1965**, *36*, 2024.
(5) Fujita, K.; Suehiro, S.; Nomura, S.; Kawai, H. *Polym. J.* **1982**, *11*, 331.
(6) Matsuo, M.; Xu, C. *Polymer* **1997**, *38*, 4311.
(7) Bin,Y.; Tanabe, Y.; Nakabayashi, C.; Kurose, H.; Matsuo, M. *Polymer* **2001**, *42*, 1183.
(8) Matsuo, M.; Bin, Y.; Nakano, M. *Polymer* **2001**, *42*, 4687.
(9) Matsuo, M.; Sato, R.; Yanagida, N.; Shimizu, Y. *Polymer* **1992**, *33*, 1640.
(10) Matsuo, M.; Sawatari, C.; Iwai, Y.; Ozaki, F. *Macromolecules* **1990**, *23*, 3266.
(11) Krigbaum, W. R.; Balta, Y. I. *J. Phys. Chem.* **1967**, *71*, 1770.
(12) Song, K. *J. Appl. Polym. Sci.* **2000**, *78*, 412.
(13) Hall, I. H.; Pass, M. G. *Polymer* **1976**, *17*, 807.
(14) Carr, P. L.; Jakeways, R.; Klein, J. L.; Ward, I. M. *J. Polym. Sci., Polym. Phys. Ed.* **1997**, *35*, 2465.
(15) Ambroziak, M.; Gruin, I.; Wronikowski, M.; Zdunek, K. *J. Appl. Polym. Sci.* **2002**, *86*, 2130.
(16) Ricco, T.; Regoretti, A. *J. Polym. Sci., Part B: Polym. Phys.* **2002**, *40*, 236.
(17) Liau, W.-B.; Liu, A. S.; Chiu, W.-Y. *Macromol. Chem. Phys.* **2002**, *203*, 294.
(18) Boye, C. A., Jr.; Overton, J. R. *Bull. Am. Phys. Soc.* **1974**, *19*, 352.
(19) Stein, R. S.; Misra, A. *J. Polym. Sci., Polym. Phys. Ed.* **1980**, *18*, 327.
(20) Matsuo, M.; Sugiura, Y.; Kimura, T.; Ogita, T. *Macromolecules* **2002**, *35*, 4493.
(21) Nomura, S.; Kawai, H.; Kimura, I.; Kagiyama, M. *J. Polym. Sci., Part A2* **1970**, *8*, 383.
(22) Matsuo, M.; Tamada, M.; Terada, T.; Sawatari, C.; Niwa, M. *Macromolecules* **1982**, *15*, 988.
(23) Sakaguchi, N.; Oda, T.; Nakai, A.; Kawai, H. *Sen-I-Gakkaishi* **1977**, *33*, 499.
(24) Wilchinsky, Z. W. *Polymer* **1964**, *5*, 271.
(25) Yokouchi, M.; Sakakibara, Y.; Chatani, Y.; Tadokoro, H.; Tanaka, T.; Yods, K. *Macromolecules* **1976**, *9*, 266.
(26) Desborough, I. J.; Hall, I. H. *Polymer* **1977**, *18*, 825.
(27) Spendly, W.; Hext, G. R.; Homsworth, F. R. *Technometrics* **1962**, *4*, 441.

(28) Kuhn, W.; Grun, F. *Kolloid-Z.* **1942**, *101*, 248.
(29) Maeda, M.; Hibi, S.; Ito, F.; Momura, S.; Kawaguhi, T.; Kawai, H. *J. Polym. Sci., Part A2* **1970**, *8*, 1303.
(30) Matsuo, M. *Macromolecules* **1990**, *23*, 3261.
(31) Stein, R. S. *J. Polym. Sci.* **1958**, *31*, 335.
(32) Nishijima, Y.; Fujimoto, T.; Onogi, Y. *Rep. Prog. Polym. Phys. Jpn.* **1966**, *9*, 457.
(33) Kimura, I.; Kagiyama, M.; Nomura, S.; Kawai, H. *J. Polym. Sci., Part A2* **1969**, *7*, 709.
(34) Pinaud, F.; Jarry, J. P.; Sergot, Ph.; Monnerie, L. *Polymer* **1982**, *23*, 1575.
(35) LeBourvellec, G.; Monnerie, L.; Jarry, P. *Polymer* **1986**, *27*, 856.

MA030347X